A Detailed Numerical Simulation of an Impulsively Started N-Dodecane Lifted Jet Flame at 40 Bar

Yuki Minamoto[1] and Jacqueline H. Chen[2]
[1] Tokyo Institute of Technology, Meguro, Tokyo, Japan
[2] Sandia National Laboratories, Livermore, CA, USA

1 Introduction

A partially premixed flame typically consists of leading fuel rich, fuel lean premixed flames and a trailing diffusion flame which consumes excess fuel and oxidizer originating from the premixed flame branches. For a given aerothermochemical condition, the so-called triple flame is stabilized at a certain distance from the jet exit, which is known as the lift-off length. Given the relevance of partially premixed combustion to lift-off stabilization of diesel engines, there has been numerous studies related to stabilization, propagation and structure associated with partially premixed flames, both experimental and numerical. In particular, previous direct numerical simulation studies have shed light on the structure and the stabilization mechanism of lifted flames for both canonical and engine-relevant thermochemical conditions.

Lifted jet flames for single-stage ignition fuels, such as hydrogen and ethylene, have been investigated in the context of DNS in previous studies [1–3], revealing that dominant stabilization mechanisms include edge flame propagation [1] and locally autoignitive mixtures that follow coherent large flow structure [3, 4], depending on the coflow temperature. More recently, lifted jet flames for two-stage ignition fuels have been studied. Although the stabilization mechanism of lifted-flames with two-stage ignition remains unclear, the conventional "triple flame structure" has been extended to include "multi-brachial" structure due to the first stage ignition process [5–7]. However, in diesel engine combustion, the onset of ignition and transition to a lifted flame yield additional complexities and the link between these previous insights on stabilized lifted flames and diesel engine combustion remains unclear. Understanding these additional complexities will provide crucial insights for the modeling of turbulent combustion in diesel combustion.

Therefore, in the present study, a detailed numerical simulation has been performed based on a direct numerical simulation code with reduced spatial resolution to capture the fundamental physics associated with ignition of a diesel jet and its transition to a lifted flame.

Correspondence to: yminamot@navier.mes.titech.ac.jp

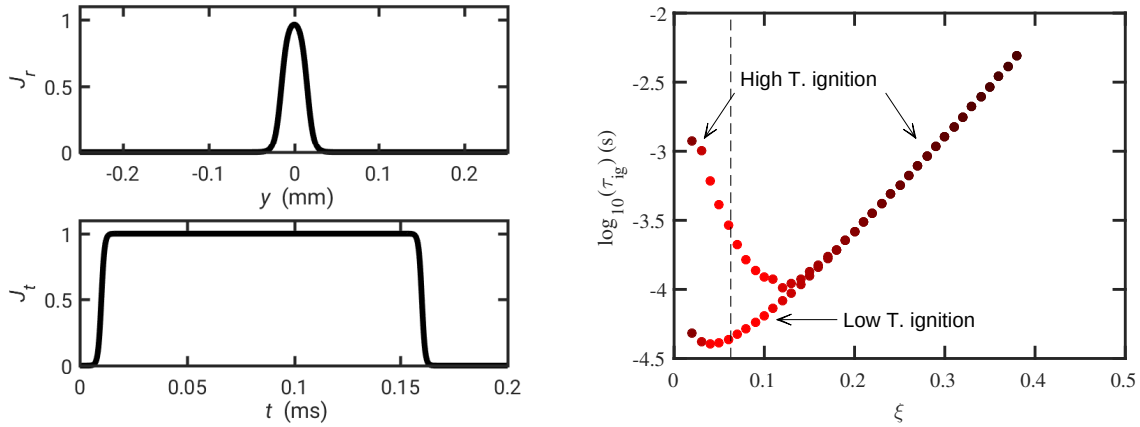

Figure 1: (a) Profiles of J_r and J_t, and (b) ignition delay versus mixture fraction ξ from a homogeneous reactor simulation, where the vertical dashed line corresponds to the stoichiometric mixture fraction.

2 Numerical Simulation

The simulation was performed using the DNS code S3D [8]. The code solves the fully-compressible conservation equations for mass, momentum, total energy and species mass fractions. The chemical reactions are described by a reduced mechanism for n-dodecane-air combustion including 35 species for both low and high temperature oxidation. The species specific heats are modeled as polynomial functions of temperature as described in CHEMKIN and TRANSPORT, and mixture-averaged transport coefficients are used [9, 10]. Radiative heat transfer is not considered in the present simulations. Spatial derivatives are obtained using an eighth-order central finite difference scheme which gradually reduces to a third-order one-sided difference stencil at the open domain boundaries [11]. A tenth-order explicit spatial filter is applied to remove any spurious high-frequency fluctuation in the solution [11]. Time integration is achieved using a six-stage fourth-order explicit Runge-Kutta method [11]. The domain dimensions are $L_x \times L_y \times L_z = 2.6 \times 1.6 \times 1.6\mathrm{mm}^3$. The domain is discretized into $N_x \times N_y \times N_z = 1040 \times 360 \times 360$ mesh points, which are non-uniform in the transverse direction as specified in a previous DNS study of a stabilized lifted jet flame [2]. The mesh size in the streamwise direction Δx is a constant value of 2.5 μm, while in the transverse and spanwise directions, Δy and Δz, vary from 2.5–12 μm. It was found that during the jet ignition process for the present thermo-chemical conditions described below, low-temperature species generate very thin structures with a thickness of 6.5 $\mu\mathrm{m}$, and with the present spatial resolution, the finest flame structure is not fully resolved. To resolve all relevant chemical scales would require a resolution of at least $0.65\mu\mathrm{m}$, which is computationally infeasible. Therefore, the present simulation resolves 1/3–1/4 of the finest scales of the reactive scalars.

The computational boundary in the streamwise direction is specified as an iso-thermal no slip wall with a temperature of 1000 K, except for the jet region as described below. Other computational boundaries are specified as non-reflecting out-flow conditions based on the Navier-Stokes Characteristic Boundary Conditions (NSCBC) method [12, 13].

At the inflow boundary ($x = 0$), the inpulsively started jet is specified for a streamwise velocity u, temperature T and species mass fractions Y_i as:

$$u(y,z) = u_{jet} J_r(y,z) J_t(t), \tag{1}$$

$$T(y,z) = (T_{jet} - T_{air}) J_r(y,z) J_t(t) + T_{air}, \tag{2}$$

$$Y_i(y,z) = (Y_{i,jet} - Y_{i,air}) J_r(y,z) J_t(t) + Y_{i,air}, \tag{3}$$

where the subscripts "*jet*" and "*air*" denote freestream values of the jet and air streams, respectively. The normalized spatial and temporal jet profiles, J_r and J_t respectively, are given as:

$$J_r = 0.5 \left[\tanh\left(\frac{r + r_{jet}}{r_{jet}\sigma_{jet}} \right) + \tanh\left(\frac{-r + r_{jet}}{r_{jet}\sigma_{jet}} \right) \right], \tag{4}$$

$$J_t = 0.25 \tanh\left[\frac{t - t_{0,jet}}{(t_{1,jet} - t_{0,jet})\tau_{tran}} \right] \tanh\left[\frac{-t + t_{1,jet}}{(t_{1,jet} - t_{0,jet})\tau_{tran}} \right], \tag{5}$$

where r is the radius from the jet center and t is the elapsed time from the beginning of the simulation. Other jet parameters used in the present study are: $u_{jet} = 45$ m/s, $T_{jet} = 400$ K, $T_{air} = 1000$ K, $r_{jet} = 0.015$mm, $\sigma_{jet} = 0.5$, $t_{0,jet} = 10$ μs, $t_{1,jet} = 150$ μs and $\tau_{tran} = 0.01$. Equations (1)–(5) prescribe the jet profiles for velocity and scalars such that they are smoothly imposed in time and space. The profiles of J_r and J_t are shown in Fig. 1a.

The fuel jet is comprised of pure n-dodecane slightly preheated to $T_{jet} = 400$ K, while air initially in the computational domain is preheated to $T_{air} = 1000$ K. The pressure is taken to be 40 atm, and note that these thermochemical parameters are relevant to diesel engine combustion. Under the present conditions, the ignition delay time of the mixture at various mixture fractions ξ is computed by using SENKIN and the results are shown in Fig. 1b. Note that the ignition delay is based on local maxima of heat release rate in time. Due to the high pressure conditions, the mixture exhibits a two-stage ignition process, and low-temperature heat release exists both in fuel lean and fuel rich mixtures, although the species mass fraction of the low-temperature species such as $C_{12}H_{25}O_2$ is very small for fuel lean conditions. The minimum ignition delay time corresponding to high-temperature ignition is comparable to the jet duration, $t_{1,jet} - t_{0,jet}$, and a similar relation between ignition delay and jet duration is observed in typical diesel engine conditions.

3 Results

Figure 2 shows general features of the lifted jet flame at different times, $t = 72$, 95 and 185 μs, where the first two times correspond to the minimum ignition delay times for homogeneous low-temperature and high-temperature ignition, respectively. The temporal and spatial evolution of ξ (Figs. 2a–2c) shows the process of mixing and the fuel containing region after fuel injection has terminated. Clearly, the mixing due to turbulent fluid motion is intense at the tip of the jet (at $x \sim 1.2$, 1.4 and 2.0 mm in Figs. 2a, 2b, 2c, respectively), even for the present low Re condition. However, due to the weak shear layers in the present flow field, shear generated turbulence is not nearly as strong as observed in [14].

The variations of $Y_{C_{12}H_{25}O_2}$ in Figs. 2d–2f show the locations of low-temperature ignition. At $t = 72$ and 95 μs, which are near the minimum ignition delay time for low-temperature ignition, there are localized low-temperature ignition processes occurring at various locations in both the shear layer and at the tip of the

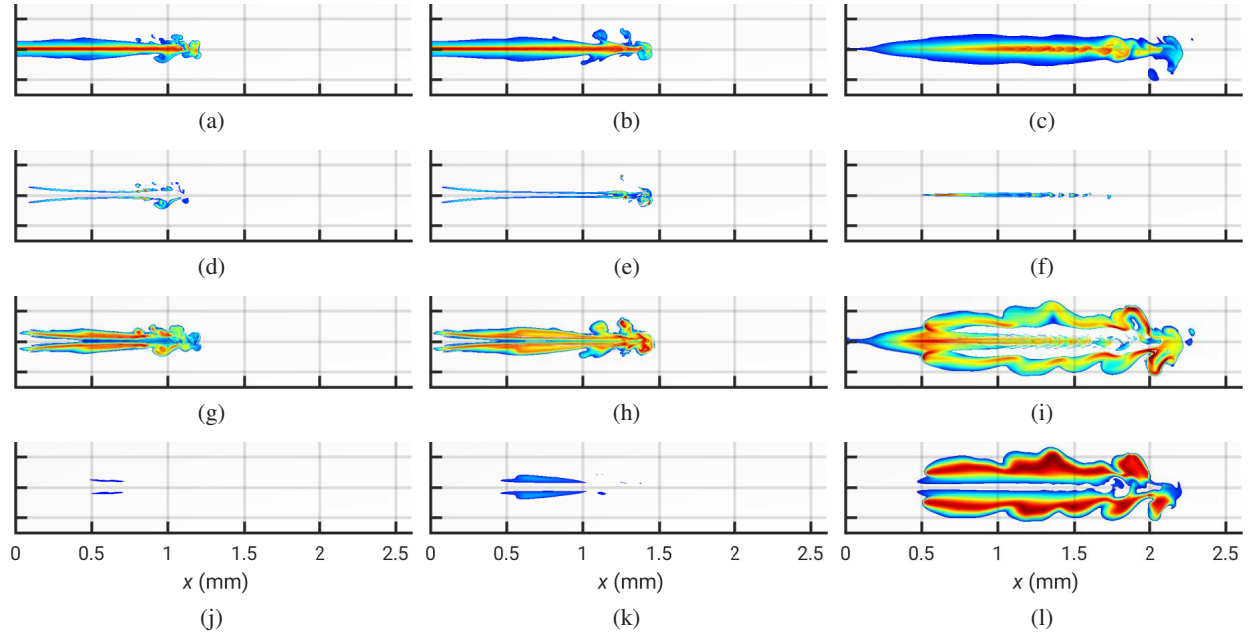

Figure 2: A spanwise mid-plane slice showing ξ (a,b,c), $Y_{C_{12}H_{25}O_2}$ (d,e,f), $\log_{10}[\max(1, Q)]$ (g,h,i), and T (j,k,l) at $t = 72$, 95 and 185 μs (first, second and third columns, respectively). The color scales (blue–red) represent the dynamic range: 0–0.8 (a, b, c), 0–0.020 (d, e, f), 9–12.5 $\log_{10}(\mathrm{J/m^3/s})$ (g, h, i) and 1000–2800 K (j, k, l).

jet, and the impulsively started jet configuration seems to generate favorable mixtures for low-temperature ignition at various locations. A similar observation has been made in a previous study of a non-reacting LES of "Spray-A" [14]. However, the maximum concentration of the low-temperature species mass fraction, corresponding to "intense" low-temperature oxidation, is located at the tip of the jet at approximately $x \sim 1.4$ mm in Fig. 2e.

One interesting observation is the structure of the reaction zones in the present jet flame compared with other stabilized lifted flames. As shown in Figs. 2g and 2h, relatively large heat release rate is observed inside the relatively high shear region, whereas the most intense heat release rate is located near the tip of the jet at approximately $x \sim 1.4$ mm in Fig. 2e. This is consistent with a previous experimental study where it was observed that the initial ignition kernel is formed at the jet tip [15]. Reiterating, low-temperature ignition is robust in the region where the concentration of low-temperature species is the highest. Therefore, high- and low-temperature igniting mixtures are entangled in this region due to the complex scalar mixing process. Following the occurrence of high-temperature ignition, a lifted flame is established with a well-known multi-brachial flame structure as shown in Fig. 2i. Since the present turbulent intensity is relatively low, turbulence is not strong enough to contort the "large-scale" flame structure; hence, the various branches are clearly delineated. The triple-point is clearly observed at $x \sim 0.5$ mm, followed by rich premixed and trailing diffusion flames downstream. The lean premixed flame branches are not evident in Fig. 2i, since the heat release rate associated with this branch is nominally two orders of magnitude smaller than the rich premixed branches [6]. Note that there are additional flame branches upstream of the triple flame, corresponding to the upstream low-temperature flame branch that has been first observed in laminar DME-

air lifted jet flames [5–7].

Figures 2j–2l shows that temperature initially increases in the shear regions for slightly lean-to-stoichiometric mixtures (observed in a conditional average $\langle T|\xi\rangle$, not shown here). As shown in Fig. 2k, the most intense heat release region (tip of the jet at approximately $x \sim 1.4$ mm) also contributes to the initial temperature increase. Eventually, the temperature variation shows a typical lifted-flame structure similar to ones observed in previous stabilized lifted flames [1, 4, 6].

4 Summary

A detailed numerical simulation of an impulsively started n-dodecane-air jet flame under diesel engine relevant conditions has been performed using a DNS code, S3D. Despite the spatial under-resolution by a factor of 3–4, the simulation results exhibit similar trends to that reported in previous numerical and experimental observations for both low- and high-temperature oxidation. The simulation results suggest that intense mixing occurs near the tip of the jet, facilitating the production of relatively intense reactions for both low- and high-temperature ignition. Moreover, the low- and high-temperature ignition processes are spatially entangled and concentrated in localized regions. The competition between these two ignition processes may be investigated by using highly-resolved direct numerical simulations [16]. After the initiation of high-temperature chemical reactions, the well-known lifted flame with a triple-point is established with additional upstream flame branches related to the low-temperature ignition. This indicates that the insights obtained in previous stabilized lifted flames may also be relevant to the unsteady lifted stabilization process of diesel engine combustion.

Acknowledgements

This research used resources of the Oak Ridge Leadership Computing Facility at the Oak Ridge National Laboratory, which is supported by the Office of Science of the U.S. Department of Energy under Contract DE-AC05-00OR22725. The work at Sandia National Laboratories was supported by NSF/DOE Partnership on Advanced Combustion Engines under Contract BET-1258646 and by the US Department of Energy, Office of Basic Energy Sciences, Division of Chemical Sciences, Geosciences, and Biosciences. Sandia is a multiprogram laboratory operated by Sandia Corporation, a Lockheed Martin Company, for the United States Department of Energy under contract DE-AC04-94AL850 00. YM acknowledges the support of the Grant-in-Aid for Young Scientists B (16K18026) of the Japan Science and Technology Agency (JST), Japan.

References

[1] Y. Mizobuchi, S. Tachibana, J. Shinjo, S. Ogawa, and T. Takeno, "A numerical analysis of the structure of a turbulent hydrogen jet lifted flame," *Proc. Combust. Inst.*, vol. 29, no. 2, pp. 2009–2015, 2002.

[2] C. S. Yoo, R. Sankaran, and J. H. Chen, "Three-dimensional direct numerical simulation of a turbulent lifted hydrogen jet flame in heated coflow: flame stabilization and structure," *J. Fluid Mech.*, vol. 640, pp. 453–481, 2009.

[3] C. S. Yoo, E. S. Richardson, R. Sankaran, and J. H. Chen, "A dns study on the stabilization mechanism of a turbulent lifted ethylene jet flame in highly-heated coflow," *Proc. Combust. Inst.*, vol. 33, no. 1, pp. 1619–1627, 2011.

[4] C. S. Yoo and H. G. Im, "Characteristic boundary conditions for simulations of compressible reacting flows with multi-dimensional, viscous reacting effects," *Combust. Theory Model.*, vol. 11, no. 2, pp. 259–286, 2007.

[5] A. Krisman, E. R. Hawkes, M. Talei, A. Bhagatwala, and J. H. Chen, "Polybrachial structures in dimethyl ether edge-flames at negative temperature coefficient conditions," *Proc. Combust. Inst.*, vol. 35, no. 1, pp. 999–1006, 2015.

[6] Y. Minamoto and J. H. Chen, "Dns of a turbulent lifted dme jet flame," *Combust. Flame*, vol. 169, pp. 38–50, 2016.

[7] S. Deng, P. Zhao, M. E. Mueller, and C. K. Law, "Autoignition-affected stabilization of laminar non-premixed DME/air coflow flames," *Combust. Flame*, vol. 162, pp. 3437–3445, 2015.

[8] J. H. Chen, A. Choudhary, B. de Supinski, M. DeVries, E. R. Hawkes, S. Klasky, W. K. Liao, K. L. Ma, J. Mellor-Crummey, N. Podhorszki, R. Sankaran, S. Shende, and C. S. Yoo, "Terascale direct numerical simulations of turbulent combustion using S3D," *Comput. Sci. Discov.*, vol. 2, pp. 1–31, 2009.

[9] R. Kee, F. Rupley, E. Meeks, and J. Miller, "Chemkin III: A Fortran chemical kinetics package for the analysis of gas-phase chemical and plasma kinetics," *Sandia National Laboratories*, vol. SAND96-8216, 1996.

[10] R. J. Kee, G. Dixon-Lewis, J. Warnatz, M. E. Coltrin, and J. A. Miller, "A Fortran computer code package for the evaluation of gas-phase multicomponent transport properties," *Sandia National Laboratories*, vol. SAND86-8246, 1986.

[11] C. A. Kennedy and M. H. Carpenter, "Several new numerical methods for compressible shear-layer simulations," *Appl. Numer. Math.*, vol. 14, no. 4, pp. 397–433, 1994.

[12] T. Poinsot and S. Lele, "Boundary conditions for direct simulations of compressible viscous flows," *J. Comput. Phys.*, vol. 101, pp. 104–129, 1992.

[13] J. C. Sutherland and C. A. Kennedy, "Improved boundary conditions for viscous, reacting, compressible flows," *J. Comput. Phys.*, vol. 191, pp. 502–524, 2003.

[14] G. Lacaze, A. Misdariis, A. Ruiz, and J. C. Oefelein, "Analysis of high-pressure diesel fuel injection processes using les with real-fluid thermodynamics and transport," *Proc. Combust. Inst.*, vol. 35, no. 2, pp. 1603–1611, 2015.

[15] M. Bardi, R. Payri, L. M. Malbec, G. Bruneaux, L. M. Pickett, J. Manin, T. Bazyn, and C. L. Genzale, "Engine combustion network: Comparison of spray development, vaporization, and combustion in different combustion vessels," *Atomization Spray*, vol. 22, no. 10, pp. 807–842, 2012.

[16] G. Borghesi and J. H. Chen, "A DNS investigation of turbulent n-dodecane jet autoignition," *Western States Section of the Combustion Institute*, March 21–22, 2016, Seattle, WA.